Protective Effect of Tricholoma Matsutake Extract on Alcoholic Liver Disease Based on Zebrafish Model

Ning-Jing Jiang [1], Yi-Mei Ding [2], Ming-Fang He [1, *]

[1] College of Biotechnology and Pharmaceutical Engineering, Nanjing Tech University, Nanjing 211816, China.

[2] Jiangsu Provincial Institute of Materia Medica, Nanjing 211816, China.

Abstract. In China, average alcohol intake and alcoholic liver disease (ALD) incidence have demonstrated escalating trends, yet the diagnostic and therapeutic infrastructure for ALD remains underdeveloped. At present, there are still some problems in the therapeutic drugs of alcoholic liver disease, such as poor therapeutic effect, obvious side effects and use restrictions. Therefore, there is a continuous need to develop new, safer, and more effective therapeutic drugs to meet clinical demands. This study, based on a zebrafish adult model of chronic ALD, the protective effects of Tricholoma matsutake (T. matsutake) extract were evaluated, and the potential mechanisms were explored. Results revealed that the extract significantly alleviated ethanol-induced hepatic lipid accumulation, restored liver architecture, normalized liver function indices, and reversed oxidative stress perturbations in adult zebrafish. Through transcriptome sequencing, the bioinformatics analysis demonstrated that T. matsutake extract exerted hepatoprotective effects against ALD by modulating key genes involved in lipid metabolism, glucose homeostasis, acetaldehyde detoxification, and oxidative stress responses. This study, based on zebrafish model, elucidated the hepatoprotective effects of T. matsutake extract against ALD, offering novel therapeutic strategies for its clinical management.

Keywords: Alcoholic liver disease; *Tricholoma matsutake* extract; Zebrafish model; Lipid metabolism.

1. Introduction

Chronic and excessive alcohol consumption leads to alcoholic liver disease (ALD). Research indicates that ALD progression involves the interplay of toxic effects from alcohol metabolites, oxidative stress, inflammatory responses, and lipid metabolic disorders. Single-target drugs often fail to comprehensively intervene in these multifaceted pathological processes. The number of ALD patients in China has been increasing annually; however, there are currently no specific therapeutic drugs available for clinical management of this condition.

Tricholoma matsutake (T. matsutake), an edible mushroom with medicinal properties, exhibits significant nutritional value, low toxicity, and minimal side effects. Existing studies demonstrate its involvement in regulating hepatic glycogen homeostasis, modulating human immunity, and maintaining redox balance[1]. Furthermore, T. matsutake extracts have been shown to exert anti-inflammatory effects by inhibiting pro-inflammatory mediators[2]. These biological activities are closely related to the pathological mechanisms of ALD, though the potential of T. matsutake extracts to reverse ALD has not yet been reported.

Zebrafish (Danio rerio) has emerged as a valuable animal model for studying human metabolic diseases and identifying potential therapeutic strategies due to its metabolic similarities to humans.

Previous studies by Park Ki-Hoon et al. established a chronic ALD model in adult zebrafish, which replicated pathological, metabolic, and stress responses observed in human ALD patients[3].

This study utilizes a zebrafish-based chronic ALD model to investigate the protective effects of T. matsutake e extracts against ALD and elucidate the underlying mechanisms. The findings aim to provide a novel therapeutic strategy for clinical ALD management.

2. Results

2.1 The effect of *T. matsutake* extract on the liver of zebrafish models

We first investigated the impact of T. matsutake extract on the liver, especially the morphology of liver and hepatocyte, in a zebrafish model. The experiment revealed that neither alcohol nor T. matsutake extract treatment resulted in alterations to the liver organ coefficient among different groups of zebrafish (Fig. 1A). Hematoxylin and eosin (H&E) staining of the zebrafish liver in each group showed that hepatocytes in the control group were neatly arranged, with large, round nuclei and tightly connected cells. In contrast, hepatocytes in the alcohol-induced model group exhibited disordered arrangement, with a significant presence of fat vacuoles, indicating severe lipid accumulation. However, treatment with T. matsutake extract ameliorated hepatic lipid accumulation and restored liver tissue structure, suggesting that T. matsutake extract rescued alcohol-induced hepatocyte damage at the microscopic level (Fig. 1B).

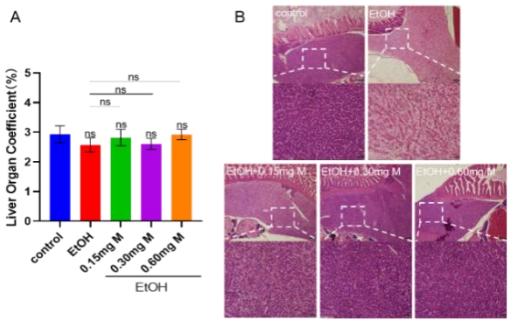

Fig. 1 Effects of *T. matsutake* extract on the liver of zebrafish model. (A) Liver coefficient of zebrafish in each group; (B) H&E staining of zebrafish liver in each group. Statistical data: ns indicated no significant differences. M stands for *T. matsutake* extract.

2.2 The effect of *T. matsutake* extract on liver function indicators in zebrafish model

Liver function indicators are common clinical examination items that reflect hepatic physiological functions. Therefore, liver function indicators were employed to evaluate the impact of T. matsutake extract on the liver function of zebrafish. Compared with the control group, the levels of aspartate aminotransferase (AST) and alanine aminotransferase (ALT) in the liver tissues of adult zebrafish in the model group were significantly elevated. In contrast, the levels of AST and ALT in the T. matsutake extract-treated groups at various concentrations were significantly reduced, indicating that it ameliorated the alcohol-induced liver function damage in zebrafish (Fig. 2).

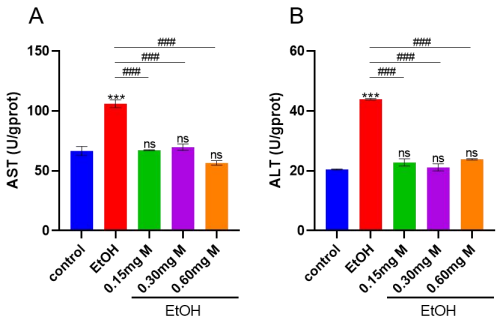

Fig. 2 Liver function detection in adult zebrafish. (A) AST and (B) ALT levels in zebrafish livers from different experimental groups. Statistical data: Compared with the control group, ***P < 0.001; Compared with the model group (EtOH), ###P < 0.001; ns indicated no significant differences. M stands for *T. matsutake* extract.

2.3 The effects of *T. matsutake* extract on oxidative stress indicators in zebrafish model

Oxidative stress plays a pivotal role in the pathogenesis of alcoholic liver disease. Therefore, detecting oxidative stress indicators is crucial for evaluating the protective effects of T. matsutake extract against alcoholic liver injury. Compared to the control group, the liver tissue of zebrafish in the model group exhibited significantly elevated superoxide dismutase (SOD) and catalase (CAT) levels. Notably, administration of T. matsutake extract at various concentrations significantly reduced SOD and CAT levels compared to the model group (Fig. 3). These findings suggest that T. matsutake extract may exert protective effects by ameliorating alcohol-induced oxidative stress.

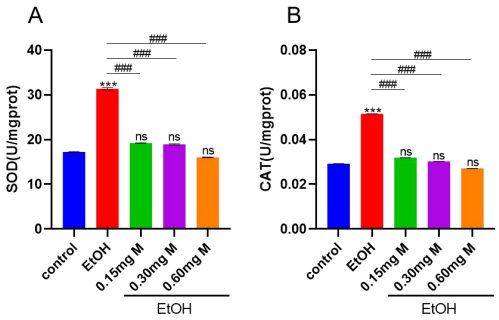

Fig. 3 Oxidative stress detection in adult zebrafish. (A) SOD and (B) CAT levels in zebrafish livers from different experimental groups. Statistical data: Compared with the control group, ***P < 0.001; Compared with the model group (EtOH), ###P < 0.001; ns indicated no significant differences. M stands for *T. matsutake* extract.

2.4 Transcriptome sequencing analysis

To investigate the hepatoprotective mechanism of T. matsutake extract, transcriptome sequencing was performed on liver tissues of adult zebrafish from three groups: normal control, alcohol-induced model (EtOH), and T. matsutake extract-treated (M). Based on gene expression profiles across samples, a clustering heatmap was generated (Fig. 4A). The EtOH group exhibited 2,544 upregulated and 4,311 downregulated differentially expressed genes (DEGs) compared to the control group (Fig. 4B), while the M group showed 4,166 upregulated and 2,885 downregulated DEGs compared to EtOH group (Fig. 4C). A Venn diagram analysis of DEGs from both comparisons (EtOH vs. control and M vs. EtOH) revealed 4,552 genes with opposing expression trends between the two contrasts (Fig. 4D).

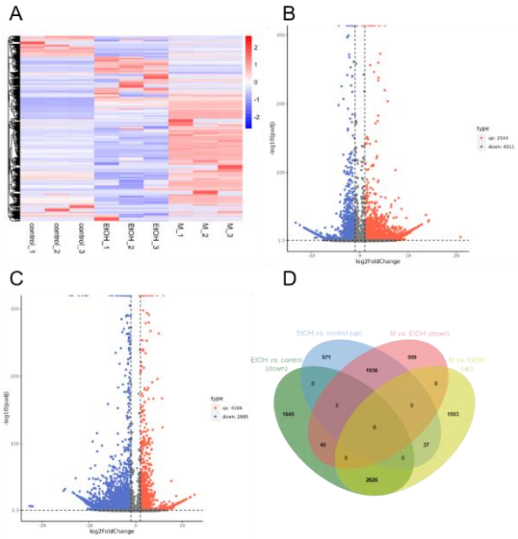

Fig. 4 Differentially expressed genes (DEGs) among the control group, model group, and *T. matsutake* extract-treated group. (A) Heatmap for clustering of DEGs in the control group, model group (EtOH) and treatment group by *T. matsutake* extract (M); (B) Volcano map of DEGs in EtOH group *vs.* control group and M group *vs.* EtOH group (C); (D) Wayne diagram of DEGs.

Gene Ontology (GO) enrichment analysis of these 4,552 DEGs indicated their involvement in biological processes such as carbohydrate metabolic process and lipid metabolic process (Fig. 5A), localization in cellular components including cytoplasm and nucleus (Fig. 5B), and molecular functions such as metal ion binding and transferase activity (Fig. 5C). Kyoto Encyclopedia of Genes and Genomes (KEGG) pathway analysis demonstrated significant enrichment in metabolic pathways including metabolic pathways, glycerophospholipid metabolism, insulin signaling pathway, starch and sucrose metabolism, pantothenate and CoA biosynthesis, and glycerolipid metabolism (Fig. 5D).

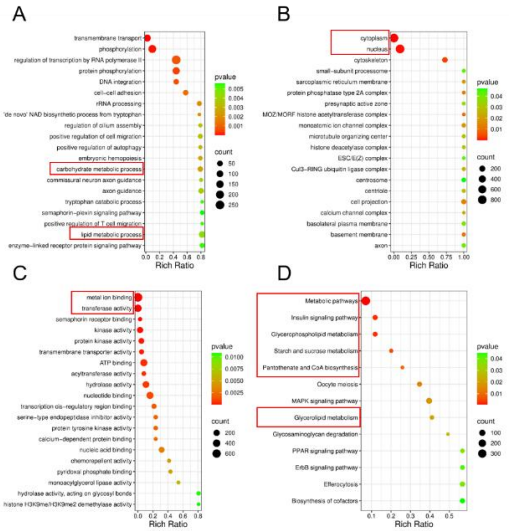

Fig. 5 Bubble graphs of GO and KEGG enrichment analysis of differentially expressed genes. Bubble graphs of GO enrichment analysis-biological process(A), cell component (B), molecular function (C); (D) Bubble graphs of KEGG enrichment analysis-signal pathway.

In the KEGG pathway enrichment analysis, the majority of significantly enriched pathways were metabolism-related (Fig. 5D). Therefore, we performed Venn diagram analysis on DEGs from the

top 5 most significant metabolic pathways identified in KEGG enrichment (Fig. 6). This analysis revealed that a subset of DEGs participated in two or more KEGG pathways. Consequently, 16 key DEGs involved in two or more KEGG pathways were screened, including dgke, ppap2d, mboat2a, agpat4, hkdc1, plpp2a, dgkaa, gpat3, pygmb, agpat9l, plpp1a, dgkh, aldh2.2, aldh3a2b, pygl, and gys2.

Fig. 6 Wayne diagram of 5 metabolic pathways in KEGG enrichment analysis.

2.5 RT-qPCR validation of differentially expressed genes

To validate the transcriptome sequencing results, the 16 selected key DEGs associated with metabolic pathways underwent RT-qPCR verification (Fig. 7). The RT-qPCR results revealed that except for the pygmb gene, the remaining 15 genes (dgke, ppap2d, mboat2a, agpat4, hkdc1, plpp2a, dgkaa, gpat3, agpat9l, plpp1a, dgkh, aldh2.2, aldh3a2b, pygl, and gys2) exhibited consistent expressions with the transcriptome sequencing results, demonstrating the reliability of the sequencing data.

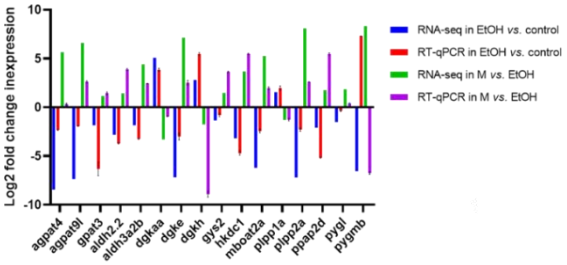

Fig. 7 Validation of RNA-Seq results by RT-qPCR.

3. Discussion

This study evaluated the protective effects of T. matsutake extract on ALD using a zebrafish adult chronic ALD model. First, we assessed changes in the liver coefficient of adult zebrafish. The results indicated that neither alcohol treatment nor T. matsutake extract administration caused significant changes in the liver coefficient of zebrafish, which differed from observations in murine models[4]. This discrepancy may arise from the relatively small liver size in zebrafish, rendering it unsuitable for liver coefficient analysis. However, H&E staining revealed severe lipid accumulation in the livers of alcohol-treated zebrafish, consistent with pathological manifestations observed in murine chronic ALD models[5], indicating microscopic pathological damage. Treatment with various concentrations of T. matsutake extract significantly ameliorated hepatic lipid accumulation and restored liver tissue architecture. Prior studies also demonstrated that T. matsutake extract

attenuated alcohol-induced acute gastric histopathological changes in murine models, showing findings analogous to those observed in the present study [6]. Subsequently, we measured hepatic functional markers (AST and ALT) across groups. The AST and ALT levels were significantly elevated in the alcohol-induced model group. Notably, T. matsutake extract treatment at all tested concentrations significantly reduced these markers, suggesting that the extract protects zebrafish from alcohol-induced liver dysfunction by improving cellular membrane integrity. Furthermore, we evaluated oxidative stress markers. The ALD model group showed significantly increased SOD and CAT levels, indicating compensatory enhancement of antioxidant enzyme activity to counteract excessive ROS accumulation. However, T. matsutake extract intervention reduced hepatic SOD and CAT levels to near-control values, suggesting that the extract may mitigate oxidative stress by directly scavenging ROS or inhibiting ROS production, thereby reducing the demand for endogenous antioxidant enzymes[7].

To investigate the protective mechanisms of T. matsutake extract against ALD, we performed transcriptome sequencing on liver tissues from control, ALD model, and T. matsutake extract-treated zebrafish. Differential gene expression analysis identified DEGs, and Venn diagram analysis revealed 4,552 DEGs with opposing expression trends between the EtOH vs. control and M (T. matsutake extract) vs. EtOH comparisons. GO and KEGG pathway enrichment analyses of these 4,552 DEGs identified significantly enriched pathways, leading to the selection of 16 key DEGs that were validated by RT-qPCR. Among these, dgkaa, dgke, dgkh, ppap2d, agpat4, agpat9l, gpat3, mboat2a, plpp1a, and plpp2a were associated with lipid metabolism[8-10]; aldh2.2 and aldh3a2b were linked to acetaldehyde metabolism and oxidative stress[11]; while pygmb, pygl, hkdc1, and gys2 were related to glucose metabolism[12]. These findings suggest that T. matsutake extract exerts hepatoprotective effects against ALD by modulating key genes involved in lipid metabolism, glucose metabolism, acetaldehyde metabolism, and oxidative stress pathways.

This study, based on a zebrafish model, demonstrates that T. matsutake extract protects against ALD potentially through regulating key genes involved in lipid metabolism and other related pathways, highlighting its therapeutic potential for ALD. However, the specific bioactive components in T. matsutake extract remain incompletely characterized. Future studies should focus on structural identification, isolation, and purification of these active components. Additionally, building on the mechanistic insights from this study, subsequent research could explore molecular targets of T. matsutake extract's active components in ALD, identify potential biomarkers, and develop novel therapeutic strategies.

4. Materials and Methods

4.1 Zebrafish maintenance

The zebrafish used in the experiment were wild-type AB strain zebrafish. They were reared in an independent, temperature-controlled fish room. The fish room was equipped with an automatic lighting system, with a daily light-dark cycle ratio of 14 h:10 h. The rearing water temperature was maintained at 28.5 ± 0.5 ℃, with a pH ranging from 7.2 to 7.6 and an electrical conductivity between 500 - 550 μS/cm.

4.2 Establishment of a chronic alcoholic liver disease model in adult zebrafish and drug administration

Adult zebrafish aged 4 - 6 months were randomly divided into three groups: the control group, the model group, and the treatment group (treated by T. matsutake extract), with 20 fish in each group. The zebrafish in the model group and the treatment group were reared in system water containing 0.2% (v/v) ethanol. The fish tanks were sealed, and the experiment lasted for 28 days. The ethanol-containing system water in the fish tanks was replaced daily. The zebrafish in the control group were reared in system water without ethanol. T. matsutake extract was incorporated into the feed. The zebrafish in the treatment group were fed with 5 mg of feed containing T. matsutake extract (0.15, 0.30, 0.60 mg) per fish per day, respectively. The zebrafish in the control and model groups were fed with the same feed without T. matsutake extract.

4.3 Calculation of liver organ coefficient

At the end of the experiment, zebrafish from each group were collected. After being euthanized by freezing on ice, the zebrafish were weighed. The liver tissues were then dissected out and weighed. The method for calculating the liver organ coefficient is shown in Equation (4-1).

$$\text{Liver organ coefficient (\%)} = \frac{\text{Liver weight(mg)}}{\text{Body weight(mg)}} \quad (4\text{-}1)$$

4.4 Hematoxylin and eosin staining

At the end of the experiment, zebrafish from each group were collected and euthanized via ice-cold immersion. The specimens were then immersed in 4% paraformaldehyde solution and stored at 4°C for overnight fixation. The fixed samples were embedded in paraffin, sectioned into 5 μm slices, and then subjected to deparaffinization, rehydration, and H&E staining. The stained sections were observed and photographed using a stereomicroscope.

4.5 Preparation of liver tissue supernatant

At the end of the experiment, zebrafish from each group were collected, euthanized, and dissected to obtain liver tissues. For each experimental group, 3 - 5 liver tissues were collected, weighed, and placed in 1.5 mL centrifuge tubes. Normal saline was added at a ratio of weight (mg): volume (μL) = 1:9. The tissues were homogenized on ice, followed by centrifugation at 4000 relative centrifugal force (rcf) for 10 minutes at 4 °C. The supernatant was then collected to obtain the liver tissue supernatant.

4.6 Detection of liver function indicators and oxidative stress indicators

The liver tissue supernatants from each experimental group were diluted to an appropriate concentration. According to the manufacturer's instructions, the activities of aspartate aminotransferase (AST) and alanine aminotransferase (ALT) were measured using AST and ALT test kits, respectively. The activities of total superoxide dismutase (T-SOD) and catalase (CAT) were determined using T-SOD and CAT assay kits, following the manufacturer's protocols. The total protein concentration, measured by the BCA protein assay kit, was used to standardize each of the detected indicators.

4.7 Transcriptome sequencing and bioinformatics analysis

Total RNA was extracted from the liver tissues of zebrafish in each group and subjected to RNA quality control (QC). Upon passing QC, mRNA enrichment and fragmentation were performed, followed by double-stranded cDNA synthesis, end repair with poly(A) tailing, and ligation of sequencing adapters. Subsequently, purification and fragment selection were carried out using magnetic beads, followed by PCR amplification to obtain the library. After passing library QC, the library was sequenced using the Illumina sequencing system. The raw sequencing data obtained were subjected to quality control using FASTQ. Based on the gene expression levels across different samples, correlation heatmaps and clustering heatmaps were generated. Differential gene expression analysis was conducted using DESeq, with the criteria for screening differentially expressed genes set as $|\log2FoldChange| > 1$ and a significance level of $padj \leq 0.05$, thereby identifying differentially expressed genes. The selected differentially expressed genes were then subjected to Gene Ontology (GO) enrichment analysis and Kyoto Encyclopedia of Genes and Genomes (KEGG) pathway enrichment analysis using the DAVID database, with a significance threshold for enrichment set at P-value < 0.05.

4.8 Real-time qPCR of key differentially expressed genes

Zebrafish liver were lysed in Trizol reagent, and total RNA was extracted according to the manufacturer's protocol. Complementary DNA (cDNA) was synthesized from the total RNA using a First-Strand cDNA Synthesis SuperMix Kit. Quantitative PCR (qPCR) analysis was performed using qPCR SYBR Green Premix. The relative expression of target genes was calculated using the 2-ΔΔCT method. The primers for each gene are listed in Table 4-1.

Table 4-3 Primer sequence of genes

Gene	Nucleotide Sequence 5’ to 3’
dgke	CGGGGTGTATGGCTCATTCC
ppap2d	ACCATGCTTTACCTGGCATTCT
mboat2a	CTCTGGCTGAAAAGGGTGTGT
agpat4	AGGCTGAGCAGTGCAACTTA
hkdc1	GCTGCCATCCTAACACGGAT
plpp2a	GGCCAAGTACACCATCGGAC
dgkaa	TGATGAAGAAGGTTTCCGCC
gpat3	CACCATCATATGGGGCCTGG
pygmb	TGTGAAGGGTTGGCAGGTAG
agpat9l	TTTCCTTCCTAACTGCAGAGTGAA
plpp1a	TCCCTGTCACTTTGCTTACTATGA
dgkh	GAGTCATCCGACAGCGAAGG
aldh2.2	GCATTTCTGCTCTGGGGATCA
aldh3a2b	TCATCAATCAGCGGCACTTCA
pygl	ATTATTTCGCGCTGTCGCAC
gys2	ACCTCCAGGCGCTATAGTAGAA
β-actin	TCGTCCACCGCAAATGCTTCTA

4.9 Data Statistics and Analysis

All experimental data were processed and analyzed using GraphPad Prism 8.4.3. The results of data analysis are presented as mean ± SEM (standard error of the mean). Significance analysis was conducted using the Dunnett's method within one-way ANOVA. A P-value less than 0.05 was considered statistically significant. (*) indicates a comparison between each group and the control group, while (#) denotes a comparison between the drug-treatment group and the model group. (***) and (###) represent $P < 0.001$, (**) and (##) represent $P < 0.01$, and (*) and (#) represent $P < 0.05$. All experimental groups were set up with three biological replicates, and each experiment was repeated at least three times.

References

[1] Li Quan, Wang Yanzhen, Cai Guangsheng, et al. Antifatigue Activity of Liquid Cultured Tricholoma matsutake Mycelium Partially via Regulation of Antioxidant Pathway in Mouse. BioMed research international, 2015, 2015: 562345.

[2] Li Mengqi, Dong Liu, Du Hanting, et al. Potential mechanisms underlying the protective effects of Tricholoma matsutake singer peptides against LPS-induced inflammation in RAW264.7 macrophages. Food chemistry, 2021, 353: 129452.

[3] Park Ki-Hoon, Kim Seok-Hyung. Low dose of chronic ethanol exposure in adult zebrafish induces hepatic steatosis and injury. Biomedicine & pharmacotherapy, 2019, 117: 109179.

[4] Guo Weiling, Cao Yingjia, You Shize, et al. Ganoderic acids-rich ethanol extract from Ganoderma lucidum protects against alcoholic liver injury and modulates intestinal microbiota in mice with excessive alcohol intake. Current Research in Food Science, 2022, 5: 515-30.

[5] Wang Yalan, Chen Qiubing, Wu Shuang, et al. Amelioration of ethanol-induced oxidative stress and alcoholic liver disease by in vivo RNAi targeting Cyp2e1. Acta pharmaceutica Sinica B, 2023, 13(9): 3906-18.

[6] Li Mengqi, Lv Renzhi, Xu Xiaomeng, et al. Tricholoma matsutake-Derived Peptides Show Gastroprotective Effects against Ethanol-Induced Acute Gastric Injury. Journal of agricultural and food chemistry, 2021, 69(49): 14985-94.

[7] Ma Ning, Tao Hongling, Du Hengjun, et al. Antifatigue effect of functional cookies fortified with mushroom powder (Tricholoma Matsutake) in mice. Journal of food science, 2020, 85(12): 4389-95.

[8] Barbernitz Xin, Raben Daniel M. Phosphorylation of DGK. Advances in biological regulation, 2023, 88: 100941.

[9] Wei Ziyi, Wang Weiguo, Xu Wenping, et al. Studies on immunotoxicity induced by emamectin benzoate in zebrafish embryos based on metabolomics. Environmental toxicology, 2024, 39(1): 97-105.

[10] Huo Huanhuan, Hu Chonghua, Zhou Qiubai, et al. Integrated transcriptome and metabolome analysis reveals a possible mechanism for the regulation of lipid metabolism via vitamin A in rice field eel (Monopterus albus). Frontiers in physiology, 2023, 14: 1254992.

[11] Singh Surendra, Brocker Chad, Koppaka Vindhya, et al. Aldehyde dehydrogenases in cellular responses to oxidative/electrophilic stress. Free radical biology & medicine, 2013, 56: 89-101.

[12] Migocka-Patrzałek Marta, Lewicka Anna, Elias Magdalena, et al. The effect of muscle glycogen phosphorylase (Pygm) knockdown on zebrafish morphology. The international journal of biochemistry & cell biology, 2020, 118: 105658.